Article

Expression of Transcription Factor ZBTB20 in the Adult Primate Neurogenic Niche under Physiological Conditions or after Ischemia

Dimo S. Stoyanov [1,†], Martin N. Ivanov [1,2,†], Tetsumori Yamashima [3] and Anton B. Tonchev [1,2,*]

[1] Department of Anatomy and Cell Biology, Faculty of Medicine, Medical University, 9000 Varna, Bulgaria
[2] Research Institute, Medical University, 9000 Varna, Bulgaria
[3] Department of Psychiatry and Behavioral Science, Kanazawa University Graduate School of Medical Sciences, Kanazawa 920-1192, Japan
*   Correspondence: anton.tonchev@mu-varna.bg
†   These authors contributed equally to this work.

Abstract: The *Zbtb20* gene encodes for a transcription factor that plays an important role in mammalian cortical development. Recently, its expression was reported in the adult mouse subventricular zone (SVZ), a major neurogenic niche containing neural stem cells throughout life. Here, we analyzed its expression in the adult primate anterior SVZ (SVZa) and rostral migratory stream (RMS) using macaque monkeys (*Macaca fuscata*). We report that the majority of Ki67+ cells, 71.4% in the SVZa and 85.7% in the RMS, co-label for ZBTB20. Nearly all neuroblasts, identified by their Doublecortin expression, were positive for ZBTB20 in both regions. Nearly all GFAP+ neural stem cells/astrocytes were also positive for ZBTB20. Analysis of images derived from a public database of gene expression in control/ischemic monkey SVZa, showed evidence for *ZBTB20* upregulation in postischemic monkey SVZa. Furthermore, the co-localization of ZBTB20 with Doublecortin and Ki67 was increased in the postischemic SVZa. Our results suggest that ZBTB20 expression is evolutionarily conserved in the mammalian neurogenic niche and is reactive to ischemia. This opens the possibility for further functional studies on the role of this transcription factor in neurogenesis in primates.

Keywords: ZBTB20; non-human primate; subventricular zone; neural progenitor

1. Introduction

The concept that neural stem cells (NSC) regenerate neurons in the adult mammalian brain is currently widely accepted [1]. The subventricular zone (SVZ) of the lateral cerebral ventricle and the subgranular zone (SGZ) of the hippocampal dentate gyrus are the two best known adult neurogenic regions (niches). Other brain regions, such as the hypothalamus, amygdala, striatum, and substantia nigra may also be able to generate new neurons throughout life [2]. The SGZ is situated adjacent to the hippocampal hillus under the dentate gyrus and is responsible for producing new dentate granule cells [1,3–5]. A minority of those newly formed neurons survive and become functionally integrated into the local circuits [6,7]. Hippocampal neurogenesis was also confirmed in monkeys and humans and persists throughout life [8–11]. The SVZ is located along the wall of the lateral ventricle [12,13]. It contains a heterogenous cell population including NSCs, transit-amplifying cells (TACs), and neuroblasts that are all at different levels of differentiation. These cell types are also known as B, C, and A cells, respectively. NSCs are able to form rapidly proliferating cells (TACs) that can give rise to immature neurons (neuroblasts) that migrate towards the olfactory bulb, forming a chain of migrating cells known as the rostral migratory stream (RMS) [12–14]. Once their final destination is reached, they mature into interneurons and functionally integrate into the

local circuitry [15]. Both SVZ and RMS seem to be preserved across mammalian species but do exhibit some structural differences. The monkey RMS appears as a well-formed hypercellular stream, exhibiting similar morphological traits to the one found in rodents, but cellular migration can be scarce [16–19]. Humans also show a preserved SVZ and an RMS, but migratory cells are so far considered to be rare at adult age [20,21]. The adult primate SVZ consists of three layers. The apical-most layer, bordering the ventricular surface, is the ependymal layer (EL). Underneath it is a hypocellular zone called the gap zone, filled with astrocytic and ependymal processes originating from the adjacent layers. Deeper than the EL is a sheet of cells, many of them astrocytes, representing the subependymal layer (SEL) [17,21–23].

Cerebral ischemia is the leading cause of damage to the brain. Ischemia can affect the proliferation and neurogenesis of NSCs in both SVZ and SGZ [24] While most studies focused on ischemia/neurogenesis use rodent models, data from non-human primate models suggest interspecies differences [25]. A number of transcription factors have been implicated in the regulation of rodent post-stroke neurogenesis [24], suggesting that this group of molecules has a pivotal role in the postischemic response of NSCs. However, the evidence on whether and how transcription factors contribute to post-stroke neurogenesis in primates are limited.

The zinc finger transcription factor Zbtb20 is expressed in the developing nervous system where its normal levels are necessary for the development of the hippocampus, neocortex, and olfactory bulb in mice [26–31]. Recent data suggests that Zbtb20 is also expressed at different stages of adult neurogenesis, forming quiescent NSCs to neuroblasts [29]. Previous research has detected *ZBTB20* mRNA expression in the monkey SVZa [32]. This prompted us to study the expression pattern of the ZBTB20 protein in macaque monkey SVZa and RMS by means of immunofluorescence. Our results suggest that ZBTB20 is expressed in most SVZ neuroblasts and in all RMS neuroblasts, which express Doublecortin (DCX+). ZBTB20 co-stains with Ki67 in proliferating cells in both SVZ and RMS. Further, nearly all astrocytes marked by expression of the Glial Fibrillary Acidic Protein (GFAP+) were also positive for ZBTB20.

2. Materials and Methods

2.1. Experimental Animals

Tissue processing and animal handling was previously described [32]. Experiments with the monkeys were approved by the Animal Care and Ethics Committee of Kanazawa University, Japan (Approval protocols AP-031498 and AP-080920). The monkeys were kept in air-conditioned cages and had free daily access to food and water. The monkeys were 4–6 years of age at the time of the experiments. Surgical procedures for inducing brain ischemia have been previously described [32].

2.2. Immunofluorescence

Histological processing was performed as previously described [32]. Antigen retrieval was achieved in a Dako PT Link Pre-Treatment Module (PT100) for 5 min at 95°C in citrate buffer (pH6) and 3 PBS washes of 10 min each followed. Bovine serum diluted 1:10 in 1% of Triton X-100/PBS was applied. The primary antibodies were diluted in bovine serum/PBS/Triton. The dilutions of the primary antibodies used were as follows: ZBTB20 (1:100; HPA016815, Sigma-Aldrich, Oakville, ON, Canada, GFAP (1:800; ab4674, Abcam, Cambridge, UK), S100β (1:100; s2532 SH-B1, Sigma-Aldrich, Oakville, ON, Canada), DCX (1:500; sc-8066, Santa Cruz, Dallas, TX, USA), NeuN (1:4000; BN90, EMD, Burlington MA, USA), and Ki67 (1:50; MIB-1 M7240, DAKO, Santa Clara, CA, USA). Following 24 h of incubation with the primary antibodies, the sections were washed in PBS 3 × 5 min and incubated for 2 h at room temperature with species-directed secondary antibody conjugated to AlexaFluor-488, AlexaFluor-647, or AlexaFluor-555 fluorochromes (Thermo Fisher Scientific, Rockford, IL, USA). All secondary antibodies were diluted in bovine/PBS/Triton at 1:300. Nuclear counter staining was achieved

with 4′,6-diamidino-2-phenylindole (DAPI) at 1:10,000 for 30 min. The negative control, created by omitting the primary antibody, was used to confirm reaction specificity.

2.3. Image Acquisition and Analysis

Motorized wide-field epifluorescence microscope Zeiss AxioImager Z.2 equipped with an AxioCam Mrm rev.3 monochrome CCD camera was used for image acquisition. Z-stacks of the entire SVZ and RMS were acquired using a 20× objective (EC Plan-Neofluar 20×/0.50 M27 at resolution of 0.322 μm/pixel) and the best focus plane was chosen for the counting. To achieve higher resolution when needed, we acquired images of target zones identified on the Z-stacks and used Apotome2.0 (ZEISS Apotome.2, White Plains, NY, USA) structured illumination and a 40× air epifluorescence objective or a 100× oil immersion objective in AxioVision SE64 Rel. 4.9.1 or ZenBlue. The obtained images were exported in .tiff format and the cells were manually counted in FiJi [33]. Statistical analysis was undertaken using R and the figure plots were produced using the package ggplot2 [34,35].

2.4. ISH Image Analysis

ISH images were derived from the Monkey-niche public database (http://monkey-niche.org/, accessed on 1 of February 2022) [32]. For the quantitative analysis of gene expression, we used the custom software Celldetekt (https://github.com/tumrod/cellDetekt, accessed on 2 of February 2022) [36]. This program segregates the input image into regions by binning adjacent pixels and classifies the binned regions in 4 groups based on the estimated level of expression: (1) regions filled with dye, (2) regions partially filled with dye, (3) regions with scattered puncta of dye, and (4) and regions with no dye [36]. We estimated the regions from classes 1 and 2 to represent areas with strong expression. Based on that, we calculated the presence of regions with strong expression in the area of interest. Then, we compared the present area with strong expression in control versus ischemic brains. EL and SEL were distinguished based on morphological characteristics such as relative thickness and cell location. EL was defined as a one-cell-thick layer adjacent to the cavity of the lateral ventricle, while SEL was a region subjacent to EL with 200 μm depth.

3. Results

3.1. ZBTB20 Is Expressed in the Macaque SVZa

On coronal brain sections through the adult monkey brain, we identified the caudate nucleus and the putamen separated from each other by fibers of the internal capsule, while the remaining were adjoined by the nucleus accumbens. This level corresponded to levels ac + 3 to ac + 5 (ac, anterior commissure) according to a stereological monkey brain atlas [37]. In the DAPI channel, we identified a stream of densely packed cells corresponding to the vertical limb of the RMS (Figure 1(a1)). In the GFAP channel, we identified astrocyte processes forming a glial canal which is used as the migratory route for the newly formed neuroblasts (Figure 1(c2)). On an adjacent section stained for DCX, we found DCX+ neuroblasts in the RMS (Figure 1(c3)). At the ventricular surface, ZBTB20 was strongly expressed in the ependymal layer while scattered cells were present in the SEL (Figure 1(b1)). ZBTB20 did not co-localize with mature neurons labeled by the marker NeuN in the striatum (Figure S1).

3.2. Immunohistochemical Characterization of ZBTB20+ Cells in Macaque SVZa

Within the EL layer, a ZBTB20 positive signal was observed in all cells with ependymal morphology, which were also positive for S100β, a calcium binding protein consistently expressed in all ependymal cells (Figure 2(c1–c4)). We next focused on the SEL which is composed of heterogeneous cell types, including parenchymal astrocytes, NSCs, TACs, and neuroblasts. GFAP is expressed by both parenchymal astrocytes and NSCs. Almost all GFAP+ cells co-expressed ZBTB20 (55 of 56 GFAP+ cells) (Figure 2(d1–d4)). We next used DCX to

identify neuroblasts in the SEL and found that 84.8% (28 of 33 DCX+ cells) of them where positive for ZBTB20 (Figure 2f). We tested whether the ZBTB20+ cell proliferated by using Ki67 to visualize proliferating cells in the SVZ, and we found that 71.4% (45 of 63 Ki67+ cells) were ZBTB20+ (Figure 2e). We investigated whether ZBTB20 was expressed in TACs, defined as Ki67+/DCX- cells in SEL. We found that 68.5% (37 of 63 cells) of the Ki67+/ZBTB20+ cells were negative for DCX, and thus most probably represented TACs (Figure S2).
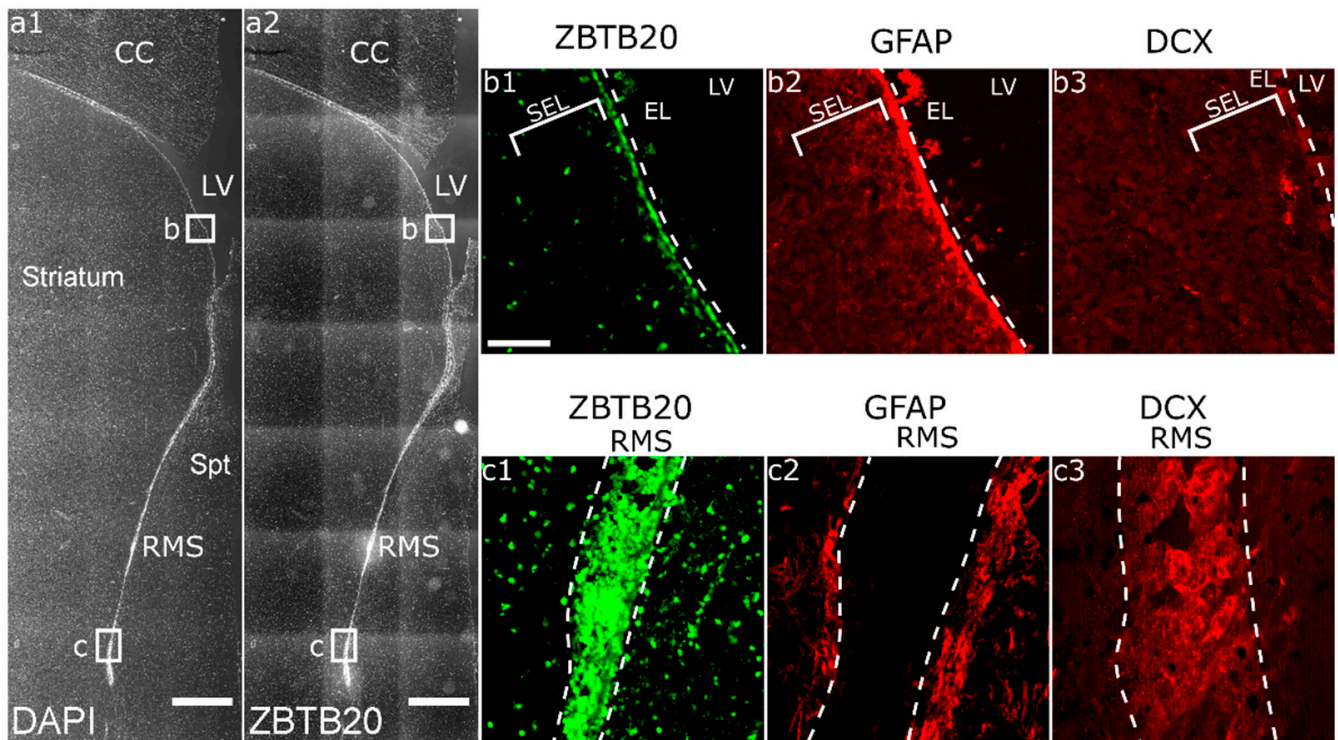

Figure 1. Overview of the ZBTB20 expression in macaque SVZa. (**a1**) DAPI staining demonstrates the major brain regions on a frontal brain section through the macaque brain. The lateral ventricle, corpus callosum, striatum, and septum are clearly identifiable. The SVZa is located on the striatal side of the lateral ventricle. RMS is well defined as a cord of densely packed cells; (**a2**) low magnification view of ZBTB20 expression on an adjacent brain section; (**b1**) higher power view of ZBTB20 expression in the SVZa; (**b2**) and (**b3**), respectively, are representative images of GFAP and DCX expression in the SVZa; (**c1**) location of ZBTB20+ cells in the RMS; (**c2**) the RMS is bordered by a sleeve of GFAP+ processes forming a glial tube; (**c3**) in the lumen of the tube, many DCX+ cells are present. EL—ependymal layer; CC—corpus callosum; LV—lateral ventricle; RMS—rostral migratory stream; Spt—septum. Scale bar: 1 mm (**a1**,**a2**).

3.3. Immunohistochemical Characterization of ZBTB20+ Cells in RMS

We identified ZBTB20+ cells both within the RMS (Figure 3(d2,e2)) and in the surrounding of the RMS (Figure 3(c2)). Upon ZBTB20/GFAP co-labeling, almost all the GFAP+ cells (20 of 21 GFAP+ cells) were ZBTB20+ (Figure 3(c1–c4)). We co-stained ZBTB20 and DCX (Figure 3(d1)), which marks migrating neuroblasts within a "canal" (glial tube) of glial cells (Figure 3(c1)). Several clusters of DCX+ cells forming a "honeycomb" pattern were observed. Due to the high cell density in this region, we applied structured illumination to subtract the out-of-focus signal and thus increase resolution. With this method we estimated that nearly all RMS DCX+ cells (77 of 79 cells) were ZBTB20+ (Figure 2d). We studied for the presence and phenotype of proliferating Ki67+ cells in the monkey RMS (Figure 2(e1)). Our analyses revealed that 85.7% (114 of 133 Ki67+ cells) were ZBTB20+ (Figure 2(e1–e4)).
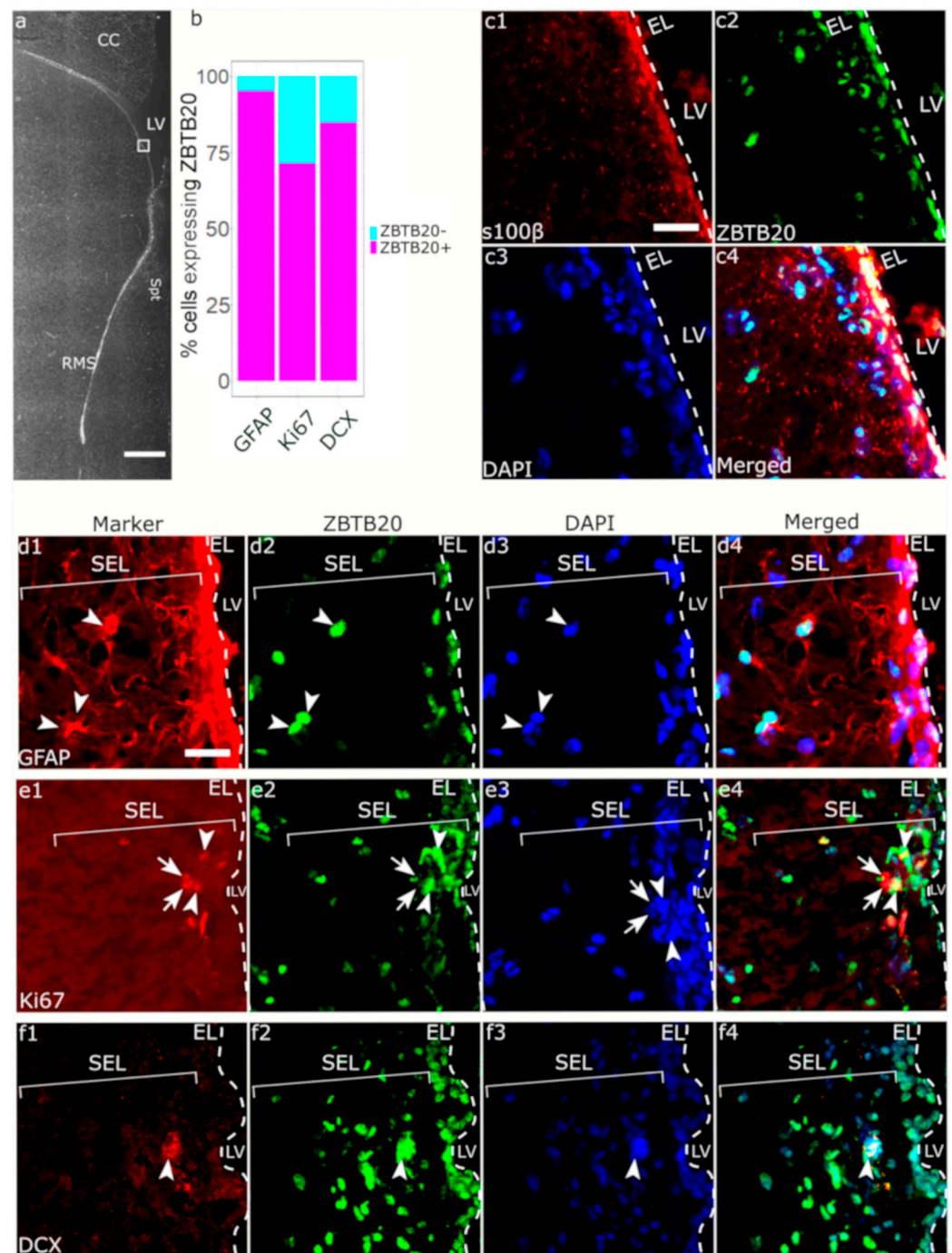
Figure 2. Phenotypic characterization of ZBTB20+ cells in the primate SVZa. (**a**) Low magnification image showing the relative position of the higher magnification micrographs in the other panels; (**b**) stacked bar plot summarizing the percentage of co-expression of ZBTB20 by specific cell populations defined by the markers shown on the plot; (**c1–c4**) the EL is defined by high s100β expression, all ependymal cells are s100β+/ZBTB20+; (**d1–d4**) most GFAP+ cells in SEL are ZBTB20+ (arrowheads); (**e1–e4**) a few Ki67+ cells can be detected in SEL, some are positive (arrowheads) or negative (arrows) for ZBTB20; (**f1–f4**) DCX+ cells were rare in SEL, arrows depict a DCX+/ZBTB20+ cell cluster. CC—corpus callosum; EL—ependymal layer; LV—lateral ventricle; RMS—rostral migratory stream; Spt—septum; SEL—subependymal layer. Scale bar: 1 mm (**a**), 25 μm (**c–f**).
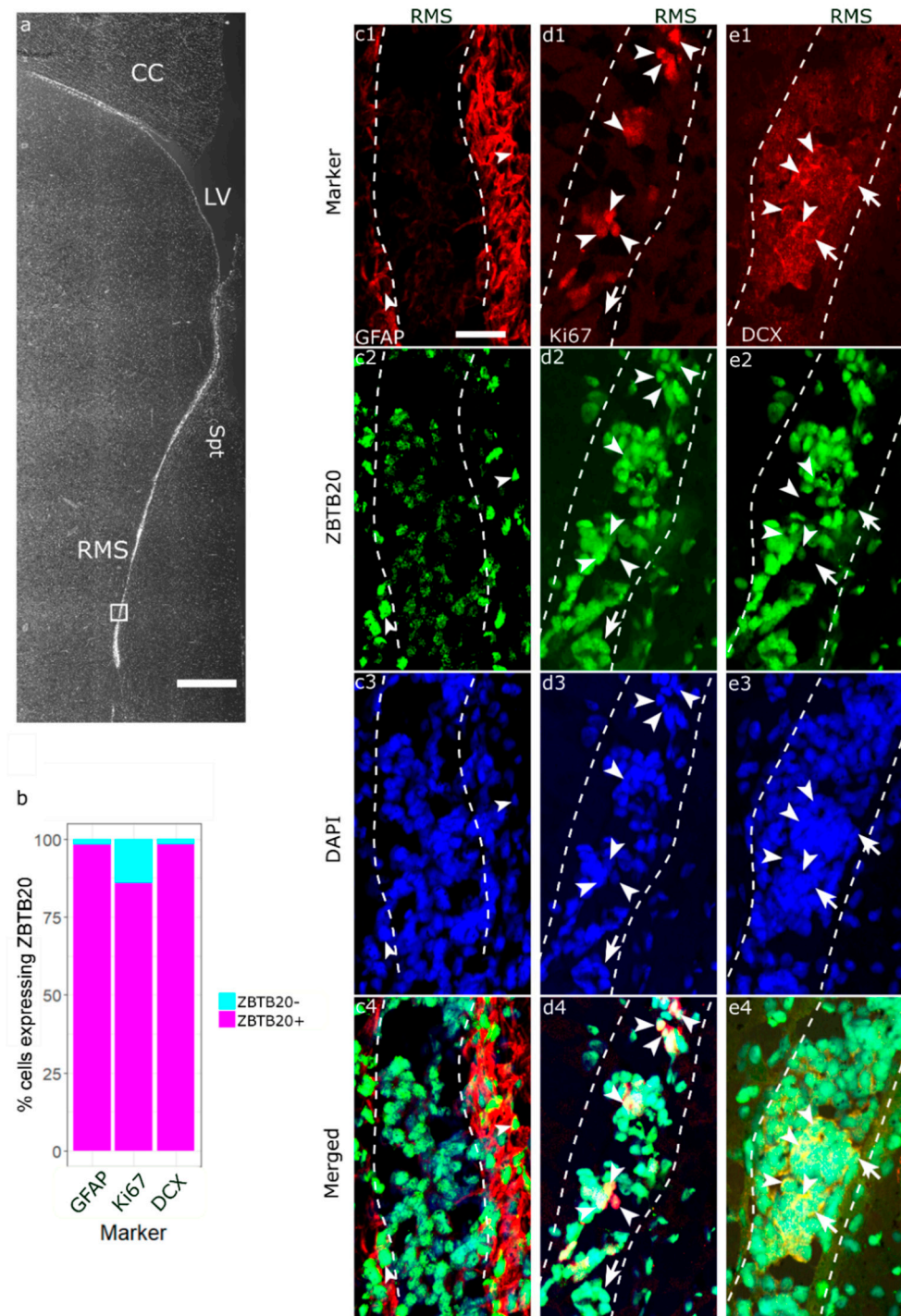
Figure 3. Phenotypic characterization of ZBTB20$^+$ cells in the primate RMS. (**a**) Low magnification image showing the relative position of the higher magnification micrographs in the other panels; (**b**) stacked bar plot summarizing the percentage of co-expression of ZBTB20 by specific cell populations defined by the markers shown on the plot; (**c1**–**c4**) arrowheads depict GFAP$^+$/ZBTB20$^+$ cells; (**d1**–**d4**) Ki67/ZBTB20 co-staining demonstrates the presence in the RMS of numerous double-labeled cells (arrowheads) and single-labeled ZBTB20 cells (arrow); (**e1**–**e4**) DCX$^+$ cells form dense clusters in the RMS exhibiting a honeycomb pattern (e1), and most co-express ZBTB20 (arrowheads). However, some DCX$^+$ cells did not co-label for ZBTB20 (arrows). CC—corpus callosum; LV—lateral ventricle; RMS—rostral migratory stream; Spt—septum. Scale bar: 1 mm (**a**), 25 μm (**c**–**e**).

3.4. Enhanced ZBTB20 mRNA Expression in the Adult Monkey SEL following an Ischemic Insult

Ischemic brain injury is a known activator of progenitor cell proliferation and neurogenesis in the macaque SVZa [38,39]. We took advantage of the public database www.monkey-niche.org [32], which shows the in situ expression of 150 genes in the adult macaque monkey SVZa under normal and ischemic conditions. Analyzing images extracted from the database, we found a striking postischemic enhancement of the *ZBTB20* mRNA in the SEL (Figure 4). Triple-labeling for ZBTB20, Ki67, and DCX in postischemic SVZa (Figure 5) revealed that all (85 of 85 cells) of the studied Ki67+ cells were ZBTB20+ (Figure 5(b1–b4,d)). Nearly all of the studied DCX+ cells (174 of 183 cells) were ZBTB20+ (Figure 5(c1–c4,d)).
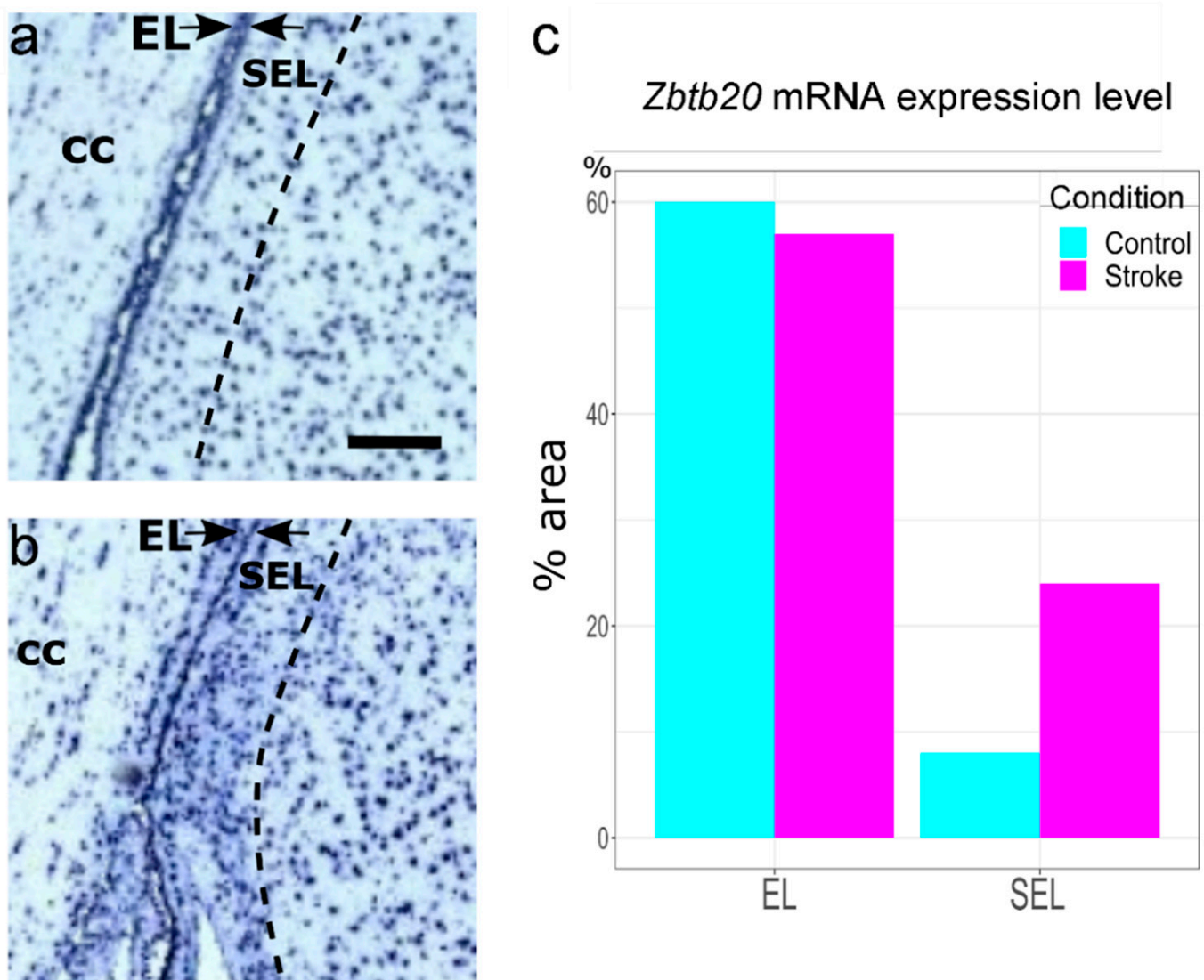

Figure 4. Increased expression of *ZBTB20* mRNA in adult macaque monkey SVZa following ischemia. (**a**) Control SVZa; (**b**) ischemic SVZa. The images were extracted from the www.monkey-niche.org public database [30]. A marked enhancement of the *ZBTB20* mRNA signal is seen in the SEL following ischemia, confirmed by quantitative assessment using the Celldetekt software (**c**). Scale = 200 µm. CC—corpus callosum.
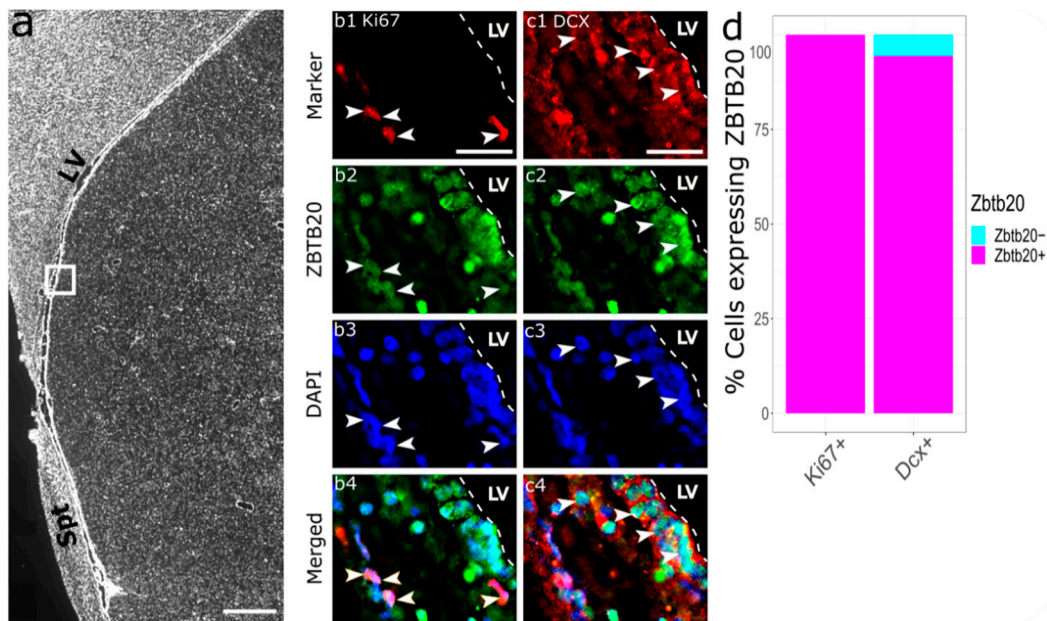
Figure 5. **Phenotypic characterization of ZBTB20+ cells in the postischemic primate SVZa.**
(**a**) Low magnification image showing the relative position of the higher magnification micrographs
panels (**b–c**); (**b1–b4**) arrowheads depict Ki67+/ZBTB20+ cells.; (**c1–c4**) DCX/ZBTB20 co-staining
demonstrates the presence of numerous double-labeled cells (arrowheads); (**d**) stacked bar plot
summarizing the percentage of ZBTB20 co-expression by specific cell populations defined by the
markers shown on the plot; CC—corpus callosum; LV—lateral ventricle; Spt—septum. Scale bar:
1 mm (**a**), 25 μm (**b,c**).

4. Discussion

Here, we report for the first time the phenotype of ZBTB20-expressing cells in adult
primate SVZa and RMS. In rodents, Zbtb20 expression in the adult SVZ progenitor cells
has been reported [29]. According to our findings, in the intact adult macaque SVZa and
RMS over 70% of the Ki67+ cells and nearly all DCX+ cells and GFAP+ cells expressed
ZBTB20. These phenotypic characteristics resemble the percentage of Zbtb20 co-expression
with Gfap, Ki67, and Dcx in the mouse, but of note is that the level of Zbtb20 protein in
Dcx+ cells in the mouse decreases as compared to levels in GFAP+ cells [29]. Outside the
neurogenic region, in the adult brain, the Zbtb20 protein was not detectable in mature
forebrain neurons in mice [40], and in this study we found a similar pattern in the monkey.

Altogether, our data demonstrate that ZBTB20 is expressed in diverse sets of niche
cells in the adult primate SVZa niche, including NSCs, TACs, and neuroblasts, but its
function remains to be identified. In the developing mouse brain, Zbtb20 loss-of-function
results in a reduced NSC proliferation [28]. Ischemia is a strong promoter of progenitor
proliferation in the monkey SVZa [38,39]. In the present study, we demonstrated enhanced
postischemic *ZBTB20* mRNA levels in parallel with an increased percentage of ZBTB20
co-expression with Ki67 and DCX. These data suggest that *ZBTB20* is candidate regulator
of primate SVZa precursor cell proliferation.

If ZBTB20 is indeed a regulator of SVZa progenitors, a number of possible mechanisms
could be implicated. Research into the function of ZBTB20 on different types of cancer cells
has revealed that in tumors, ZBTB20 positively regulates migration, tissue invasion, and
proliferation [41–43]. An important mechanism for achieving its proliferative effects might
come from the fact that ZBTB20 promotes the expression of the receptor for epidermal
growth factor (EGFR), at least in hepatocytes [44]. In the context of adult neurogenesis,
EGFR promotes the exit of NSC from quiescence and directs them toward activation and
transformation into TACs, maintaining their division potential [45–47]. Further mecha-

nistic experiments are required to prove a ZBTB20-EGFR link in the regulation of adult neurogenesis in primate SVZa.

References

1.　Obernier, K.; Alvarez-Buylla, A. Neural Stem Cells: Origin, Heterogeneity and Regulation in the Adult Mammalian Brain. *Development* **2019**, *146*, dev156059. [CrossRef] [PubMed]

2.　Jurkowski, M.P.; Bettio, L.K.; Woo, E.; Patten, A.; Yau, S.-Y.; Gil-Mohapel, J. Beyond the Hippocampus and the SVZ: Adult Neurogenesis Throughout the Brain. *Front. Cell. Neurosci.* **2020**, *14*, 576444. [CrossRef] [PubMed]

3.　Pilz, G.-A.; Bottes, S.; Betizeau, M.; Jörg, D.J.; Carta, S.; Simons, B.D.; Helmchen, F.; Jessberger, S. Live Imaging of Neurogenesis in the Adult Mouse Hippocampus. *Science* **2018**, *359*, 658–662. [CrossRef] [PubMed]

4.　Abbott, L.C.; Nigussie, F. Adult Neurogenesis in the Mammalian Dentate Gyrus. *Anat. Histol. Embryol.* **2020**, *49*, 3–16. [CrossRef]

5.　Anacker, C.; Hen, R. Adult Hippocampal Neurogenesis and Cognitive Flexibility—Linking Memory and Mood. *Nat. Rev. Neurosci.* **2017**, *18*, 335–346. [CrossRef]

6.　Kempermann, G.; Song, H.; Gage, F.H. Neurogenesis in the Adult Hippocampus. *Cold Spring Harb. Perspect. Biol.* **2015**, *7*, a018812. [CrossRef]

7.　van Praag, H.; Schinder, A.F.; Christie, B.R.; Toni, N.; Palmer, T.D.; Gage, F.H. Functional Neurogenesis in the Adult Hippocampus. *Nature* **2002**, *415*, 1030–1034. [CrossRef]

8.　Eriksson, P.S.; Perfilieva, E.; Björk-Eriksson, T.; Alborn, A.-M.; Nordborg, C.; Peterson, D.A.; Gage, F.H. Neurogenesis in the Adult Human Hippocampus. *Nat. Med.* **1998**, *4*, 1313–1317. [CrossRef]

9.　Knoth, R.; Singec, I.; Ditter, M.; Pantazis, G.; Capetian, P.; Meyer, R.P.; Horvat, V.; Volk, B.; Kempermann, G. Murine Features of Neurogenesis in the Human Hippocampus across the Lifespan from 0 to 100 Years. *PLoS ONE* **2010**, *5*, e8809. [CrossRef]

10.　Boldrini, M.; Fulmore, C.A.; Tartt, A.N.; Simeon, L.R.; Pavlova, I.; Poposka, V.; Rosoklija, G.B.; Stankov, A.; Arango, V.; Dwork, A.J.; et al. Human Hippocampal Neurogenesis Persists throughout Aging. *Cell Stem Cell* **2018**, *22*, 589–599.e5. [CrossRef]

11.　Dennis, C.V.; Suh, L.S.; Rodriguez, M.L.; Kril, J.J.; Sutherland, G.T. Human Adult Neurogenesis across the Ages: An Immunohistochemical Study. *Neuropathol. Appl. Neurobiol.* **2016**, *42*, 621–638. [CrossRef] [PubMed]

12.　Huang, Z.; Wang, Y. In Vivo Electroporation and Time-Lapse Imaging of the Rostral Migratory Stream in Developing Rodent Brain. *Curr. Protoc. Neurosci.* **2019**, *87*, e65. [CrossRef] [PubMed]

13.　Mizrak, D.; Levitin, H.M.; Delgado, A.C.; Crotet, V.; Yuan, J.; Chaker, Z.; Silva-Vargas, V.; Sims, P.A.; Doetsch, F. Single-Cell Analysis of Regional Differences in Adult V-SVZ Neural Stem Cell Lineages. *Cell Rep.* **2019**, *26*, 394–406.e5. [CrossRef]

14.　Bressan, C.; Saghatelyan, A. Intrinsic Mechanisms Regulating Neuronal Migration in the Postnatal Brain. *Front. Cell. Neurosci.* **2021**, *14*, 620379. [CrossRef] [PubMed]

15.　Wallace, J.L.; Wienisch, M.; Murthy, V.N. Development and Refinement of Functional Properties of Adult-Born Neurons. *Neuron* **2017**, *96*, 883–896.e7. [CrossRef] [PubMed]

16.　Pencea, V.; Bingaman, K.D.; Freedman, L.J.; Luskin, M.B. Neurogenesis in the Subventricular Zone and Rostral Migratory Stream of the Neonatal and Adult Primate Forebrain. *Exp. Neurol.* **2001**, *172*, 1–16. [CrossRef]

17. Sawamoto, K.; Hirota, Y.; Alfaro-Cervello, C.; Soriano-Navarro, M.; He, X.; Hayakawa-Yano, Y.; Yamada, M.; Hikishima, K.; Tabata, H.; Iwanami, A.; et al. Cellular Composition and Organization of the Subventricular Zone and Rostral Migratory Stream in the Adult and Neonatal Common Marmoset Brain. *J. Comp. Neurol.* **2011**, *519*, 690–713. [CrossRef]

18. Kornack, D.R.; Rakic, P. The Generation, Migration, and Differentiation of Olfactory Neurons in the Adult Primate Brain. *Proc. Natl. Acad. Sci. USA* **2001**, *98*, 4752–4757. [CrossRef]

19. Bédard, A.; Lévesque, M.; Bernier, P.J.; Parent, A. The Rostral Migratory Stream in Adult Squirrel Monkeys: Contribution of New Neurons to the Olfactory Tubercle and Involvement of the Antiapoptotic Protein Bcl-2: The Rostral Migratory Stream in Adult Primates. *Eur. J. Neurosci.* **2002**, *16*, 1917–1924. [CrossRef]

20. Wang, C. Identification and Characterization of Neuroblasts in the Subventricular Zone and Rostral Migratory Stream of the Adult Human Brain. *Cell Res.* **2011**, *21*, 17. [CrossRef]

21. Sanai, N.; Tramontin, A.D.; Barbaro, N.M.; Gupta, N.; Kunwar, S.; Lawton, M.T.; McDermott, M.W.; Parsa, A.T.; Verdugo, J.M.-G.; Berger, M.S.; et al. Unique Astrocyte Ribbon in Adult Human Brain Contains Neural Stem Cells but Lacks Chain Migration. *Nature* **2004**, *427*, 5. [CrossRef] [PubMed]

22. Gil-Perotin, S.; Duran-Moreno, M.; Belzunegui, S.; Luquin, M.R.; Garcia-Verdugo, J.M. Ultrastructure of the Subventricular Zone in Macaca Fascicularis and Evidence of a Mouse-Like Migratory Stream. *J. Comp. Neurol.* **2009**, *514*, 533–554. [CrossRef] [PubMed]

23. Quiñones-Hinojosa, A.; Chaichana, K. The Human Subventricular Zone: A Source of New Cells and a Potential Source of Brain Tumors. *Exp. Neurol.* **2007**, *205*, 313–324. [CrossRef] [PubMed]

24. Marques, B.L.; Carvalho, G.A.; Freitas, E.M.M.; Chiareli, R.A.; Barbosa, T.G.; Di Araújo, A.G.P.; Nogueira, Y.L.; Ribeiro, R.I.; Parreira, R.C.; Vieira, M.S.; et al. The Role of Neurogenesis in Neurorepair after Ischemic Stroke. *Semin. Cell Dev. Biol.* **2019**, *95*, 98–110. [CrossRef]

25. Tonchev, A.B.; Yamashima, T.; Sawamoto, K.; Okano, H. Transcription Factor Protein Expression Patterns by Neural or Neuronal Progenitor Cells of Adult Monkey Subventricular Zone. *Neuroscience* **2006**, *139*, 1355–1367. [CrossRef]

26. Rosenthal, E.H.; Tonchev, A.B.; Stoykova, A.; Chowdhury, K. Regulation of Archicortical Arealization by the Transcription Factor Zbtb20. *Hippocampus* **2012**, *22*, 2144–2156. [CrossRef]

27. Nielsen, J.V.; Thomassen, M.; Møllgård, K.; Noraberg, J.; Jensen, N.A. Zbtb20 Defines a Hippocampal Neuronal Identity Through Direct Repression of Genes That Control Projection Neuron Development in the Isocortex. *Cereb. Cortex* **2014**, *24*, 1216–1229. [CrossRef]

28. Tonchev, A.B.; Tuoc, T.C.; Rosenthal, E.H.; Studer, M.; Stoykova, A. Zbtb20 Modulates the Sequential Generation of Neuronal Layers in Developing Cortex. *Mol. Brain* **2016**, *9*, 65. [CrossRef]

29. Doeppner, T.R.; Herz, J.; Bähr, M.; Tonchev, A.B.; Stoykova, A. Zbtb20 Regulates Developmental Neurogenesis in the Olfactory Bulb and Gliogenesis After Adult Brain Injury. *Mol. Neurobiol.* **2019**, *56*, 567–582. [CrossRef]

30. Medeiros de Araújo, J.A.; Barão, S.; Mateos-White, I.; Espinosa, A.; Costa, M.R.; Gil-Sanz, C.; Müller, U. ZBTB20 Is Crucial for the Specification of a Subset of Callosal Projection Neurons and Astrocytes in the Mammalian Neocortex. *Development* **2021**, *148*, dev196642. [CrossRef]

31. Wang, A.; Wang, J.; Tian, K.; Huo, D.; Ye, H.; Li, S.; Zhao, C.; Zhang, B.; Zheng, Y.; Xu, L.; et al. An Epigenetic Circuit Controls Neurogenic Programs during Neocortex Development. *Development* **2021**, *148*, dev199772. [CrossRef] [PubMed]

32. Chongtham, M.C.; Wang, H.; Thaller, C.; Hsiao, N.-H.; Vachkov, I.H.; Pavlov, S.P.; Williamson, L.H.; Yamashima, T.; Stoykova, A.; Yan, J.; et al. Transcriptome Response and Spatial Pattern of Gene Expression in the Primate Subventricular Zone Neurogenic Niche After Cerebral Ischemia. *Front. Cell Dev. Biol.* **2020**, *8*, 584314. [CrossRef]

33. Schindelin, J.; Arganda-Carreras, I.; Frise, E.; Kaynig, V.; Longair, M.; Pietzsch, T.; Preibisch, S.; Rueden, C.; Saalfeld, S.; Schmid, B.; et al. Fiji: An Open-Source Platform for Biological-Image Analysis. *Nat. Methods* **2012**, *9*, 676–682. [CrossRef] [PubMed]

34. Ginestet, C. Ggplot2: Elegant Graphics for Data Analysis: Book Reviews. *J. R. Stat. Soc. Ser. A* **2011**, *174*, 245–246. [CrossRef]

35. R Core Team. *R: A Language and Environment for Statistical Computing*; R Foundation for Statistical Computing: Vienna, Austria, 2013.

36. Carson, J.P.; Eichele, G.; Chiu, W. A Method for Automated Detection of Gene Expression Required for the Establishment of a Digital Transcriptome-Wide Gene Expression Atlas. *J. Microsc.* **2005**, *217*, 275–281. [CrossRef] [PubMed]

37. Saleem, K.S.; Logothetis, N. *A Combined MRI and Histology Atlas of the Rhesus Monkey Brain in Stereotaxic Coordinates*; Elsevier/AP: Amsterdam, The Netherlands; Boston, MA, USA, 2012; ISBN 978-0-12-385088-1.

38. Tonchev, A.B.; Yamashima, T.; Zhao, L.; Okano, H.J.; Okano, H. Proliferation of Neural and Neuronal Progenitors after Global Brain Ischemia in Young Adult Macaque Monkeys. *Mol. Cell. Neurosci.* **2003**, *23*, 292–301. [CrossRef]

39. Koketsu, D.; Furuichi, Y.; Maeda, M.; Matsuoka, N.; Miyamoto, Y.; Hisatsune, T. Increased Number of New Neurons in the Olfactory Bulb and Hippocampus of Adult Non-Human Primates after Focal Ischemia. *Exp. Neurol.* **2006**, *199*, 92–102. [CrossRef]

40. Nagao, M.; Ogata, T.; Sawada, Y.; Gotoh, Y. Zbtb20 Promotes Astrocytogenesis during Neocortical Development. *Nat. Commun.* **2016**, *7*, 11102. [CrossRef]

41. Kan, H.; Huang, Y.; Li, X.; Liu, D.; Chen, J.; Shu, M. Zinc Finger Protein ZBTB20 Is an Independent Prognostic Marker and Promotes Tumor Growth of Human Hepatocellular Carcinoma by Repressing FoxO1. *Oncotarget* **2016**, *7*, 14336–14349. [CrossRef]

42. Zhang, Y.; Zhou, X.; Zhang, M.; Cheng, L.; Zhang, Y.; Wang, X. ZBTB20 Promotes Cell Migration and Invasion of Gastric Cancer by Inhibiting IκBα to Induce NF-KB Activation. *Artif. Cells Nanomed. Biotechnol.* **2019**, *47*, 3862–3872. [CrossRef]

43. Zhao, J.; Ren, K.; Tang, J. Zinc Finger Protein ZBTB20 Promotes Cell Proliferation in Non-Small Cell Lung Cancer through Repression of FoxO1. *FEBS Lett.* **2014**, *588*, 4536–4542. [CrossRef] [PubMed]

44. Zhang, H.; Shi, J.-H.; Jiang, H.; Wang, K.; Lu, J.-Y.; Jiang, X.; Ma, X.; Chen, Y.-X.; Ren, A.-J.; Zheng, J.; et al. ZBTB20 Regulates EGFR Expression and Hepatocyte Proliferation in Mouse Liver Regeneration. *Cell Death Dis.* **2018**, *9*, 462. [CrossRef] [PubMed]

45. Romano, R.; Bucci, C. Role of EGFR in the Nervous System. *Cells* **2020**, *9*, 1887. [CrossRef]

46. Llorens-Bobadilla, E.; Zhao, S.; Baser, A.; Saiz-Castro, G.; Zwadlo, K.; Martin-Villalba, A. Single-Cell Transcriptomics Reveals a Population of Dormant Neural Stem Cells That Become Activated upon Brain Injury. *Cell Stem Cell* **2015**, *17*, 329–340. [CrossRef] [PubMed]

47. Codega, P.; Silva-Vargas, V.; Paul, A.; Maldonado-Soto, A.R.; DeLeo, A.M.; Pastrana, E.; Doetsch, F. Prospective Identification and Purification of Quiescent Adult Neural Stem Cells from Their In Vivo Niche. *Neuron* **2014**, *82*, 545–559. [CrossRef]